

Cluster state generation using van der Waals and dipole-dipole interactions in optical lattices

Elena Kuznetsova,^{1,2} T. Bragdon,^{1,2} Robin Côté,¹ and S. F. Yelin^{1,2}

¹*Department of Physics, University of Connecticut, Storrs, CT 06269*

²*ITAMP, Harvard-Smithsonian Center for Astrophysics, Cambridge, MA 02138*

(Dated: July 28, 2019)

We present a scalable method for generation of a cluster state for measurement-based quantum computing using van der Waals or dipole-dipole interactions between neutral atoms or polar molecules in an optical lattice. Nearest neighbor entanglement is accomplished by performing a phase gate using interaction of atoms in Rydberg states or molecules in large dipole moment states. All nearest neighbors are sequentially entangled in a finite number of operations, independent of the number of qubits, producing a 1D cluster state. A universal 2D cluster state can be generated in several ms in a two-dimensional optical lattice by producing a series of 1D cluster states in one lattice direction, followed by application of the entangling operations in another lattice direction. We discuss the viability of the scheme with Rb Rydberg atoms.

PACS numbers:

I. INTRODUCTION

Entanglement plays a major role in quantum computing [1], quantum communication [2] and quantum metrology [3]. A special type of a multipartite entangled state, cluster state, represents a universal resource for the measurement-based quantum computing (MBQC) paradigm [4]. In measurement-based quantum computing, quantum computations are carried out on the cluster state through individual qubit measurements in adaptive bases $(|0\rangle \pm e^{i\phi}|1\rangle)/\sqrt{2}$. The primary advantage of MBQC over other register-based architectures rests in the fact that all interactions, required *e.g.* for two-qubit gates, are performed in the initialization stages of the resource state. The computation may then be performed through simultaneous measurement of many individual qubits as warranted by the specific program being implemented. Any one- and two-qubit gate can be realized by appropriate measurements, making MBQC equivalent to the standard quantum circuit model [5]. Moreover, since the actual computation is done by local measurements, it can be faster compared to the equivalent gates in the circuit model.

The cluster state is realized by preparing individual qubits in an eigenstate $|+\rangle = (|0\rangle + |1\rangle)/\sqrt{2}$ of the Pauli spin operator σ_x , and letting the nearest neighbor qubits interact via an Ising (up to local operations) Hamiltonian $H_{\text{int}} = g(t) \sum_{\langle a,a'\rangle} \frac{1-\sigma_z^{(a)}}{2} \frac{1-\sigma_z^{(a')}}{2}$ during a time τ so that $\int_0^\tau g(t)dt = \pi$. It clearly shows that the cluster state can be generated by applying a phase gate $U_{\text{PG}} = \text{diag}(1, 1, 1, -1)$ between all nearest neighbor qubits.

A cluster state was experimentally realized with photons [6] using linear optics, but this approach is difficult to scale to a large number of qubits. Schemes to generate a cluster state using atom-cavity entanglement in the framework of cavity QED [7], cold ions via phonon-mediated spin-spin interactions [8], and distributed net-

works of collectively excited atomic ensembles [9] have also been proposed. A naturally highly scalable system is neutral atoms in an optical lattice, where a 1D cluster state has been produced via ultracold s-wave collisions of atoms in a spin-dependent lattice [10]. Neutral atoms can also be entangled via long-range van der Waals (vdW) or dipole-dipole interaction when excited to Rydberg states. Atoms in Rydberg states can have huge dipole moments of several kiloDebyes and interact strongly with each other [11], which was suggested as a tool to produce two-qubit gates in neutral-atom based quantum computing [12, 13]. Recently, in a series of experiments [14] Rydberg (dipole) blockade between two atoms has been observed, followed by the demonstrations of a blockade-assisted CNOT gate [15] and entanglement between two atoms [16]. It is interesting to explore the possibility to use the strong interaction in Rydberg states to generate a cluster state. Moreover, it would offer a way to produce a cluster state with polar molecules, coupled via dipole-dipole interaction, for which collision-based interactions can result in undesirable inelastic or chemical reaction losses. For simplicity we primarily discuss in this work neutral atoms interacting in Rydberg states, the same scheme can be applied to molecules.

We propose to realize a cluster state by applying a phase gate to pairs of nearest neighbor atoms in an optical lattice. The phase gate can be realized using either direct or blockaded interaction in Rydberg states. The cluster state is generated by applying the phase gate in parallel to nearest neighbors in a lattice, in several iterations. First, atoms in each pair in some subset get entangled in one operation; next, the phase gate can be applied to pairs not touched in the first step, etc. until all nearest neighbor pairs are entangled. This scheme is scalable, *i.e.* it requires a finite number of operations, not depending on the number of atoms in the lattice. In fact, to make pair excitation controllable and to minimize errors due to interactions of multiple atoms in Rydberg states, it already suffices to excite every other pair. This

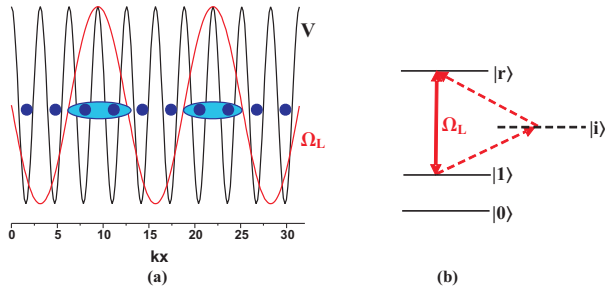


FIG. 1: (a) An optical lattice described by the potential $V = V_0 \cos^2(kx)$, along with an excitation pulse in the form of a standing wave with Rabi frequency $\Omega_L = \Omega_{L0} \cos^2(kx/4 + \phi)$, where $\phi = \pi/4$; (b) Atoms are conditionally transferred from *e.g.* a qubit state $|1\rangle$ to a Rydberg state $|r\rangle$ by optical one or two-photon π -pulses.

can be done using optical standing wave excitation as is illustrated in Fig. 1a in the case of a 1D optical lattice. Pairs of atoms at the maxima of the standing wave intensity will get entangled, while those at the minima will not. Changing the phase of the standing wave fields, *i.e.* shifting the position of the intensity maxima and minima, will allow to perform the phase gate between all nearest neighbors, producing a cluster state.

The paper is organized as follows. In Section II we describe how a 1D cluster state can be realized using interaction in Rydberg states. In Section III we show how to generalize the technique used for the 1D cluster state generation to produce a universal 2D cluster state. Finally, we conclude in Section IV.

II. 1D CLUSTER STATE GENERATION

We start by analyzing how a 1D cluster state can be generated by applying the phase gate between all neighboring atoms in a 1D optical lattice.

A. Phase gate without individual addressing

1. Gate analysis

We assume that initially atoms are loaded into the ground motional state of an optical lattice described by a potential $V(x) = V_0 \cos^2(kx)$, shown in Fig. 1a, which can be done using a superfluid-Mott insulator transition. Two ground state hyperfine sublevels $|F, m_F\rangle$ encode qubit states $|0\rangle$, $|1\rangle$. As a final preliminary step atoms are transferred into the $|+\rangle = (|0\rangle + |1\rangle)/\sqrt{2}$ superposition by applying a $\pi/2$ pulse, resonant with the qubit transition. A phase gate between atoms in neighboring sites can be implemented using strong vdW or dipole-dipole interaction in Rydberg states.

There are two ways to perform the phase gate depending on whether atoms are individually addressable or not [12]. Standard Rydberg blockade requires individual addressing of the atoms. Individual addressing in an optical lattice has been demonstrated recently using a tightly focused laser beam and a spin-dependent lattice [17]. However, sequential application of the phase gate to each pair of atoms in a lattice is not scalable to a large number of qubits. In a good scalable approach the cluster state has to be generated in a finite number of operations which does not depend on the size of the system. Below we analyze the possibility to generate the 1D cluster state assuming that atoms in each pair are not addressed individually.

If one uses a standing wave excitation pulse with the Rabi frequency $\Omega_L = \Omega_{L0} \cos^2(kx/4 + \phi)$, one has the maxima at *e.g.* even and minima at odd pairs sites (see Fig. 1a). The atoms are transferred from the qubit state $|1\rangle$ to the Rydberg state $|r\rangle$ either directly or by a two-photon excitation, as shown in Fig. 1b. The phase gate is realized in the limit $\Omega_L \gg V_{\text{int}}$ (V_{int} is the Rydberg interaction strength) as follows: 1) a π -pulse is applied simultaneously to both atoms exciting each from the state $|1\rangle$ to the $|r\rangle$ state, since the shift of the doubly excited state $|rr\rangle$ is smaller than the Rabi frequency; 2) atoms in the $|rr\rangle$ state interact during time T_{int} and accumulate a π phase shift $V_{\text{int}}T_{\text{int}} = \pi$; 3) a second π -pulse deexcites atoms back to their original qubit states. The standing wave therefore allows to control the Rydberg excitation pattern, which is more difficult in the case of a spatially homogeneous excitation. We also note that vdW and dipole-dipole interactions of Rydberg atoms are long-range. As a result, when atoms are excited, the interaction strength between atoms in neighboring pairs is comparable to the interaction strength between atoms within a pair, which will result in a phase error. The error is considerably reduced by exciting atoms only in every other pair using the standing wave. The interaction strength between atoms in closest excited even pairs is then smaller by a factor of $1/3^6 \sim 10^{-3}$ for vdW and $1/3^3 \sim 3.7 \cdot 10^{-2}$ for dipole-dipole interaction than the interaction strength within a pair.

Excitation to Rydberg states of alkali atoms is typically a two-photon process via intermediate $p_{1/2}$, $p_{3/2}$ states. Using the level scheme shown in Fig. 2a we can write the Schrödinger equation for the amplitudes of the qubit states. If the qubit is initially in the $|11\rangle$ state, the corresponding system of equations is

$$\begin{aligned} i \frac{da_{11}}{dt} &= -\frac{2\Omega_1^2}{\Delta} a_{11} - \frac{\Omega_1 \Omega_2}{\Delta} a_+, \\ i \frac{da_+}{dt} &= -\frac{\Omega_1^2 + \Omega_2^2}{\Delta} a_+ - \frac{2\Omega_1 \Omega_2}{\Delta} a_{11} - \frac{2\Omega_1 \Omega_2}{\Delta} a_{rr}, \\ i \frac{da_{rr}}{dt} &= (V_{\text{int}} - \frac{2\Omega_2^2}{\Delta}) a_{rr} - \frac{\Omega_1 \Omega_2}{\Delta} a_+, \end{aligned}$$

where a_{11} , a_+ and a_{rr} are the amplitudes of the states $|11\rangle$, $|+\rangle = (|1r\rangle + |r1\rangle)/\sqrt{2}$ and $|rr\rangle$ (other states are far-

detuned and not populated provided that $\Delta \gg \Omega_1, \Omega_2$; Δ is the detuning from the intermediate state, $\Omega_{1,2}$ are the Rabi frequencies of the excitation pulses). Assuming $\Omega_1 = \Omega_2 = \Omega$ and $V_{\text{int}} \ll \Omega^2/\Delta$ the solution of this system is given by

$$|\Psi\rangle = e^{2i\Omega^2 t/\Delta} \left(\frac{|11\rangle - |rr\rangle}{2} + \frac{|11\rangle - 2|+\rangle + |rr\rangle}{4} e^{2i\Omega^2 t/\Delta} + \frac{|11\rangle + 2|+\rangle + |rr\rangle}{4} e^{-2i\Omega^2 t/\Delta} \right),$$

which shows that for a pulse duration T such that $\Omega^2 T/\Delta = \pi/2$ the state evolves into $|\Psi\rangle = |rr\rangle$. Next, the excitation pulses are switched off and the atoms interact in the doubly excited state for time T_{int} so that $V_{\text{int}} T_{\text{int}} = \pi$, and the state flips sign $|\Psi\rangle = -|rr\rangle$. Finally, we apply the same π -pulse for time T , bringing the system into a state $|\Psi\rangle = -|11\rangle$.

If the initial state is $|01\rangle$ the system evolution is governed by equations (similar for the $|10\rangle$ state)

$$\begin{aligned} i \frac{da_{01}}{dt} &= -\Omega_1^2 \left(\frac{1}{\Delta} + \frac{1}{\Delta + \Delta_{\text{hf}}} \right) a_{01} - \frac{\Omega_1 \Omega_2}{\Delta} a_{0r}, \\ i \frac{da_{0r}}{dt} &= - \left(\frac{\Omega_2^2}{\Delta} + \frac{\Omega_1^2}{\Delta + \Delta_{\text{hf}}} \right) a_{0r} - \frac{\Omega_1 \Omega_2}{\Delta} a_{01}, \end{aligned}$$

which in the case $\Delta \gg \Delta_{\text{hf}}$ gives the solution

$$|\Psi\rangle = e^{2i\Omega^2 t/\Delta} \left(\frac{|01\rangle - |0r\rangle}{2} e^{-i\Omega^2 t/\Delta} + \frac{|01\rangle + |0r\rangle}{2} e^{i\Omega^2 t/\Delta} \right)$$

where Δ_{hf} is the hyperfine splitting of the atomic ground state. One can see that for $\Omega^2 T/\Delta = \pi$ the system returns to the state $|\Psi\rangle = -|01\rangle$.

Finally, if the system is initially in the $|00\rangle$ state, the wavefunction evolves as $|\Psi\rangle = e^{2\Omega^2/(\Delta + \Delta_{\text{hf}})} |00\rangle$, bringing the system into $|\Psi\rangle = |00\rangle$ for $\Omega^2 T/\Delta = \pi$ if $\Delta \gg \Delta_{\text{hf}}$. As a result, the phase gate $|\epsilon_1 \epsilon_2\rangle \rightarrow e^{i\pi(1-\epsilon_1)(1-\epsilon_2)} |\epsilon_1 \epsilon_2\rangle$ is implemented.

To proceed with cluster state generation the phase gate has to be performed with odd pairs of atoms. The phase ϕ of the excitation pulse is shifted by $\pi/2$ to become $\phi = 3\pi/4$. At this point all atoms in even and odd pairs become entangled. As a next step the phase gate has to be applied to neighboring atoms, where one atom belongs to an even and another to an odd pair, which can be done by setting $\phi = \pi/2$ and, finally, to $\phi = \pi$. This will result in the phase gate applied to all nearest neighbors.

In Fig. 2b we show the level scheme of ^{87}Rb which we use as an example. A qubit can be encoded into $|0\rangle = |F=1, m_F=0\rangle$ and $|1\rangle = |F=2, m_F=0\rangle$ states, providing long coherence lifetimes due to small sensitivity to magnetic field fluctuations [18]. A Rydberg state $ns_{1/2}$ with $|F=2, m_F=2\rangle$ can be used as $|r\rangle$, in this case atoms will interact via isotropic vdW $V_{\text{int}} = C_6/r^6$

interaction. Atoms can be excited to $|r\rangle$ using two σ^+ polarized pulses via intermediate $p_{1/2}$ ($|F=1, 2, m_F=1\rangle$) states. Assuming $\Delta = 100$ GHz, $V_{\text{int}} = 1$ MHz and $\Omega = 100$ MHz, resulting in a two-photon Rabi frequency $\Omega^2/\Delta = 10$ MHz, the total gate time is expected to be $T_{\text{PG}} = 2T + T_{\text{int}} = 2\pi/\Omega^2/\Delta + \pi/V_{\text{int}} \approx 2 \times 25 + 500 = 550$ ns. Since the phase gate pulses have to be applied four times to entangle all nearest neighbors the total time required to generate the cluster state is $2.2 \mu\text{s}$.

2. Gate errors

Let us now discuss phase gate errors. The main errors are caused by the finite width of the ground motional state wavefunction of each atom in a lattice site, which results in a finite spread of the Rabi frequency of the standing wave excitation pulse and a spread of V_{int} . Less important sources of error are the decay of population in Rydberg states and the finite ratio of the interaction strength to the two-photon Rabi frequency. In order to find the error due to the finite width of the ground state motional wavefunction we approximate the potential at each site as harmonic with the oscillation frequency $\omega = k\sqrt{2V_0/m}$ and the corresponding wavefunction width $a = \sqrt{\sqrt{E_R/V_0}/k} \approx 0.316/k$ for $V_0 = 100E_R$, which we use for an estimate. Here $E_R = \hbar^2 k^2/2m$ is the atomic recoil energy. We assume the Rabi frequencies of the excitation pulses $\Omega_1 = \Omega_2 = \Omega \sim \cos(kx/4 + \pi/4)$, where x varies around potential minima of the n^{th} even well $x_n = 5\pi/2(7\pi/2) + 4\pi n$ with the Gaussian probability distribution $p(x) = \exp(-(x - x_n)^2/a^2)/\sqrt{\pi}a$. The resulting fidelity of the phase gate is $F = \langle |\langle \Psi_0 | \Psi \rangle|^2 \rangle = 1 - \epsilon = 1 - (2 + 3\pi^2/4) \langle (\delta\Omega/\Omega)^2 \rangle - (1/8 + 27\pi^2/1024) (V_{\text{int}}/\Omega^2/\Delta)^2 - \pi\gamma/2V_{\text{int}} - 3\pi^2/16 \langle (\delta V_{\text{int}}/V_{\text{int}})^2 \rangle - 3\pi^2/16 \langle \delta V_{\text{int}}/\Omega^2/\Delta \rangle - 5\pi^2/4 \langle \delta\Omega\delta V_{\text{int}}/\Omega V_{\text{int}} \rangle$, where $|\Psi_0\rangle = |00\rangle + |01\rangle + |10\rangle - |11\rangle$ is the ideal two-qubit final state after the phase gate, ϵ is the corresponding gate error, and averaging is over the motional ground state wavefunction. The first error term is due to the spread of the Rabi frequency experienced by each atom in a pair; the second term comes from the finite ratio of the interaction strength and the two-photon Rabi frequency; the third term is due to the finite lifetime of the Rydberg state, and the last three terms are caused by the uncertainty of the interaction strength. Let us discuss the origin of this uncertainty in more detail. When two atoms originally in the ground motional states $|g_1, g_2\rangle$ and qubit states $|i_1, i_2\rangle$ are transferred to a doubly excited Rydberg state $|r_1, r_2\rangle$, the state $|g_1, g_2\rangle \otimes |r_1, r_2\rangle$ is no longer an eigenstate of the total Hamiltonian, including vdW or dipole-dipole interaction. The interaction admixes higher energy motional states to the original ground state as well as other Rydberg states to a much smaller extent. As a result, new eigenstates are superpositions of several motional and Rydberg states. If the atoms are excited to Rydberg states adiabatically, the $|g_1, g_2\rangle \otimes |r_1, r_2\rangle$ state will gradually evolve

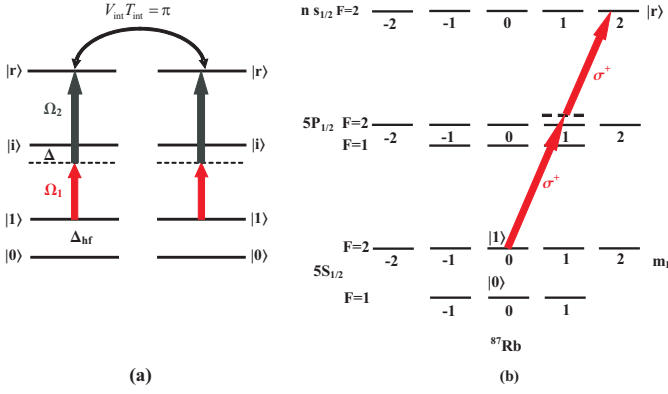


FIG. 2: (a) Two-photon excitation from the $|11\rangle$ to the $|rr\rangle$ state in alkalis; (b) Level scheme of ^{87}Rb showing qubit $|0\rangle$, $|1\rangle$ and Rydberg $|r\rangle$ states.

into an eigenstate of the total Hamiltonian. The phase accumulated during the time atoms spend in Rydberg states is then $\theta = ET_{\text{int}}/\hbar$, where E is the corresponding eigenenergy. In this case there is no uncertainty in the interaction strength (and the accumulated phase θ), provided the eigenenergy E is known and the atoms are resonantly transferred to the corresponding eigenstate. If the excitation is non-adiabatic, the atoms remain in the $|g_1, g_2\rangle \otimes |r_1, r_2\rangle$ state, which is now a superposition of several eigenstates of the total Hamiltonian. If we now calculate the average value of the interaction strength as $V_{\text{int}} = \langle g_1, g_2 | \langle r_1, r_2 | \hat{V}_{\text{int}} | g_1, g_2 \rangle | r_1, r_2 \rangle$ there will be an uncertainty of the order of $\langle (\delta V_{\text{int}}/V_{\text{int}})^2 \rangle \sim (a/R)^4 (V_{\text{int}}/\hbar\omega)^2$, where $R = \lambda/2$ is the lattice period. For $a/R = 2a/\lambda \sim 0.1$, $V_{\text{int}} \sim 1$ MHz and $\omega \sim 100$ kHz the resulting uncertainty is $\gtrsim 10^{-2}$. The contributions of the first three error terms are $(2 + 3\pi^2/4)\langle (\delta\Omega/\Omega)^2 \rangle \sim 6.3 \cdot 10^{-3}$, $(1/8 + 27\pi^2/1024)(V_{\text{int}}/\Omega^2/\Delta)^2 \sim 3.8 \cdot 10^{-4}$, $\pi\gamma/2V_{\text{int}} \sim 5 \cdot 10^{-4}$ for the Rydberg state lifetime 500 μs , *i.e.* the total error is of the order of $7.2 \cdot 10^{-3}$ if there is no uncertainty in the interaction strength and $\gtrsim 10^{-2}$ in the presence of the uncertainty. To avoid the uncertainty error the excitation has to be adiabatic with respect to the motional frequency of the lattice, which is $\omega \sim 100$ kHz in deep lattices, *i.e.* the excitation pulse duration has to be $T \gg 1/\omega \sim 1$ μs . Assuming $T \sim 10$ μs and $T_{\text{int}} = \pi/V_{\text{int}} \sim 0.5$ μs , the total gate duration is $T_{\text{PG}} \sim 20$ μs .

This analysis shows that first, vdW interaction results in smaller errors caused by the interaction of atoms in different excited pairs compared to the dipole-dipole one ($1/3^6$ compared to $1/3^3$). Second, the excitation to Rydberg states has to be adiabatic to avoid errors due to the uncertainty of the interaction strength. On the other hand, these errors can be avoided altogether if excitation to the $|rr\rangle$ state is not required. Next we therefore analyze the phase gate based on Rydberg (dipole) blockade, where only one atom is excited to a Rydberg state, provided individual addressing of atoms in a pair is possible.

B. Phase gate with "individual" addressing: dipole blockade

1. Gate analysis

If individual addressing of atoms in a pair is possible, one can use standard dipole blockade [12], and the phase gate is realized in the limit $\Omega_L \ll V_{\text{int}}$ as follows: 1) a control atom is excited from one of the qubit states, *e.g.* a qubit state $|1\rangle$ to a Rydberg state $|r\rangle$ by a π -pulse; 2) a 2π -pulse of the same frequency is applied to a target atom. Dipole-dipole or vdW interaction shifts the energy of the doubly excited state $|rr\rangle$, as a result the 2π -pulse has no effect on the target atom (the excitation is blocked) since the Rabi frequency of the pulse is much smaller than the energy shift; 3) the control atom is deexcited back to its original qubit state. We stress that we do not require individual addressing of atoms in the lattice, we only need atoms in each pair to be separately addressable, this is why we call it "individual" addressing.

Individual addressing in a pair can be realized using a polarization gradient optical lattice [19], where not only the intensity of the lattice field but also its polarization changes periodically in space. A lattice of double-wells was demonstrated in [20] with the polarization being linear in one site and elliptical in the neighboring site of each well. The elliptical polarization results in a non-zero contribution from a vector part of polarizability, producing a state-dependent shift $\sim \alpha_v(\vec{E}_L^* \times \vec{E}_L)\vec{F}$, where α_v is the vector part of the polarizability, \vec{F} is the atomic angular momentum, and \vec{E}_L is the positive frequency part of the total electric field $\vec{E} = \vec{E}_L e^{-i\omega t} + c.c.$. The contribution from the vector part can, therefore, be viewed as a fictitious magnetic field $\vec{B}_{\text{fict}} \sim \alpha_v(\vec{E}_L^* \times \vec{E}_L)$.

Atoms can be loaded into a double-well optical lattice, formed by two standing wave fields of different polarizations. Let us consider the lattice field

$$\vec{E}_L = E_0 \vec{e}_y e^{ikx+i\phi} + E_0 \vec{e}_y e^{-ikx-i\phi} + iE_1 \vec{e}_z e^{2ikx} + iE_1 \vec{e}_z e^{-2ikx}.$$

This lattice can be produced by two pairs of laser beams, intersecting at π and $\pi/3$ angles [21]. The corresponding lattice potential is a sum of scalar and vector parts $V = -\alpha_s |\vec{E}_L|^2/4 + i\alpha_v(\vec{E}_L^* \times \vec{E}_L)\vec{F}/4 = V_s + V_v$, where α_s is the scalar polarizability. The scalar part $V_s = V_0 \cos^2(kx + \phi) + V_1 \cos^2 2kx$ represents a double-well lattice, with a spatial period $a = \pi/k$; the minima of the n^{th} double-well are at $(kx_{\text{min}})_n = (\arcsin(V_0/4V_1)/2 + \pi/4 + \pi n, -\arcsin(V_0/4V_1)/2 + \pi/4 + \pi(2n+1)/2)$. The vector part is given by $V_v = -2\alpha_v \sqrt{V_0 V_1} \cos 2kx \cos kx F_x / \alpha_s$, and at the minima of a double-well $V_v = \pm \alpha_v \sqrt{V_0 V_1 (1 - V_0/4V_1)} / 2V_0 F_x / 2V_1 \alpha_s$. Here the \pm signs refer to the left and right sites of the well. The scalar part of the potential is typically larger than the vector part, since the vector polarizability is about

an order of magnitude smaller than the scalar part for alkalis. Assuming $\alpha_v/\alpha_s \sim 0.1$, $V_0 = V_1$ and $V_0 = 100E_R$ the vector shift at the well's minima is $V_v \approx \pm 3E_RF_x$. If we encode a qubit into magnetic field sensitive states, *e.g.* $|0\rangle = |F=1, m_F=-1\rangle$, $|1\rangle = |F=2, m_F=1\rangle$, the V_v term will shift states $|0\rangle$, $|1\rangle$ in the right site with respect to the qubit states in the left site of the well [22] (see Fig. 3b), allowing to selectively excite only one atom in each pair, while having another atom unaffected by the excitation pulse. For ^{87}Rb $E_R = 3.5$ kHz at the lattice wavelength $\lambda = 810$ nm, and the shifts for the $|0\rangle$, $|1\rangle$ states are $\Delta_{\text{vec}} \sim \pm 10$ kHz. Larger shifts of the order of 50–100 kHz [22] can be realized with optimized parameters of the lattice. If the two-photon excitation Rabi frequency $\Omega^2/\Delta \sim 10$ kHz (*i.e.* much smaller than the vector shift, which we take $\Delta_{\text{vec}} = 100$ kHz for an estimate), the atoms in the left and right sites can be excited to the $|r\rangle$ state selectively. The phase gate then can be realized using dipole blockade as: 1) a π -pulse resonant to the $|1\rangle - |r\rangle$ transition of a control atom is applied, exciting it to the $|r\rangle$ state; a target atom is off-resonant by $2|\Delta_{\text{vec}}|$, which is the relative shift of the qubit state $|1\rangle$ in left and right site, and is not excited; 2) a 2π -pulse resonant to the $|1\rangle - |r\rangle$ transition of the target atom is applied. The doubly excited $|rr\rangle$ state is shifted by the large interaction energy V_{int} and is not populated. The control atom is off-resonant by $2|\Delta_{\text{vec}}|$ and is not affected; 3) finally, a π -pulse resonant to the control atom brings it back to its original qubit state. These steps are summarized in the table below, which shows the evolution of the two-qubit states:

$$\begin{array}{l}
|00\rangle \xrightarrow{\pi_{\xi}} -|00\rangle \xrightarrow{2\pi_{\xi}} -|00\rangle \xrightarrow{\pi_{\xi}} |00\rangle, \\
|01\rangle \xrightarrow{\pi_{\xi}} -|01\rangle \xrightarrow{2\pi_{\xi}} |01\rangle \xrightarrow{\pi_{\xi}} -|01\rangle, \\
|10\rangle \xrightarrow{\pi_{\xi}} -i|r0\rangle \xrightarrow{2\pi_{\xi}} -ie^{i\theta}|r0\rangle \xrightarrow{\pi_{\xi}} -e^{i\theta}|10\rangle, \\
|11\rangle \xrightarrow{\pi_{\xi}} -i|r1\rangle \xrightarrow{2\pi_{\xi}} -ie^{i\theta}|r1\rangle \xrightarrow{\pi_{\xi}} -e^{i\theta}|11\rangle,
\end{array} \quad (1)$$

where $\theta = \pi|\Delta_{\text{vec}}|/\Omega^2/\Delta$, and the first qubit corresponds to the control and the second to the target atom. One can see that the phase gate can be realized provided that $\theta = 2\pi n$.

2. Gate errors

The fidelity of the phase gate with blockade $\langle F \rangle = 1 - \epsilon = 1 - 2\pi^2\langle(\delta\Omega/\Omega)^2\rangle - \pi\gamma/\Omega^2/\Delta - (1/8 + 3\pi^2/256)(\Omega^2/\Delta V_{\text{int}})^2 - (7/8 + 19\pi^2/64)(\Omega^2/2\Delta|\Delta_{\text{vec}}|)^2$ no longer contains error terms related to the uncertainty of the interaction strength. The resulting errors are $2\pi^2\langle(\delta\Omega/\Omega)^2\rangle = \pi^2(ka)^2 \left(1 - \sqrt{(1 + V_0/4V_1)/2}\right) / \left(1 + \sqrt{(1 + V_0/4V_1)/2}\right) \sim 0.15$, $\pi\gamma/\Omega^2/\Delta \sim 2.5 \cdot 10^{-2}$, $(1/8 + 3\pi^2/256)(\Omega^2/\Delta V_{\text{int}})^2 \sim 10^{-6}$, $(7/8 + 19\pi^2/64)(\Omega^2/2\Delta|\Delta_{\text{vec}}|)^2 \sim 0.16$, where we assumed $1/\gamma = 500 \mu\text{s}$, the two-photon Rabi frequency $\Omega^2/\Delta = 40$

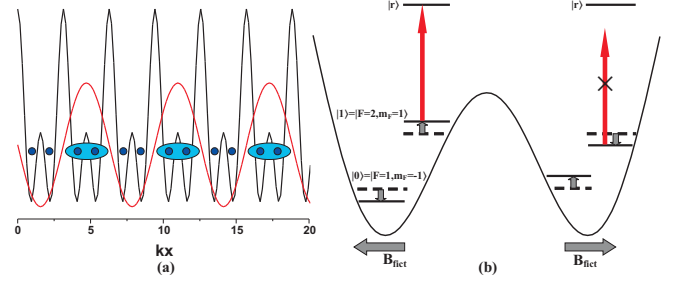


FIG. 3: (a) Double-well lattice described by the potential $V = V_0 \cos^2 kx + V_1 \cos^2 2kx$ ($V_1 = V_0$) along with a standing wave excitation pulse with Rabi frequency $\Omega_L = \Omega_{L0} \cos^2(kx/2 + \pi/4)$; (b) Shift of qubit states $|0\rangle = |F=1, m_F=-1\rangle$ and $|1\rangle = |F=2, m_F=1\rangle$ in left and right sites of a double-well in a polarization gradient lattice described in the text.

kHz, $V_{\text{int}} = 10$ MHz and the vector shift of the qubit states $\Delta_{\text{vec}} = 100$ kHz. It shows that the total error of the phase gate in this case is 0.335 and the phase gate time is $T_{PG} = 4\pi/\Omega^2/\Delta \sim 50 \mu\text{s}$. By changing the phase of the standing wave so that intensity maxima shift to odd double-wells the phase gate can be realized in odd pairs. At this stage all pairs in double-wells are entangled. In the next subsection we describe how the phase gate can be realized with neighboring atoms belonging to different double-wells.

Finally, let us discuss the error due to undesirable excitation of atoms in "inactive" wells, where the Rabi frequency is close to a minimum. During the control π and target 2π pulses the error phase $\xi \sim \pi\Omega_{\text{min}}/\Omega_{\text{max}}$ accumulates, where $\Omega_{\text{max}(\text{min})} = \left(1 \pm \sqrt{(1 + V_1/4V_0)/2}\right)$ are the Rabi frequencies experienced by atoms in active (inactive) double-wells. Then the probability to find the pair in the initial qubit state after the phase gate, averaged over four possible two-qubit states, is $\langle P \rangle = 1 - \xi^2$. For $V_0 = V_1$ $\langle P \rangle \approx 0.865$ in the case of two-photon excitation to Rydberg states. This probability can be significantly increased using multi-photon excitation pulses. For example, in the case of a four-photon excitation $\langle P \rangle \approx 0.998$.

It was shown in [24] that fault-tolerant MBQC can be realized with a 3D cluster state using topologically protected gates. In particular, an error threshold for an entangling two-qubit gate during the preparation of the cluster state has been calculated as $7.5 \cdot 10^{-3}$. The phase gate without individual addressing analyzed in Section IIA can be done with a total error of $7.2 \cdot 10^{-3}$, *i.e.* the gate error is below the threshold value, provided the excitation to an eigenstate of the total Hamiltonian is adiabatic. The phase gate error with individual addressing via dipole blockade considered in this subsection is 0.335, which is two orders of magnitude higher than the threshold. The error term $\sim (\Omega^2/2\Delta|\Delta_{\text{vec}}|)^2$ can be reduced by increasing the relative qubit energy shift $2|\Delta_{\text{vec}}|$ between left and right

sites in a double well. One possible way to increase Δ_{vec} is to use hyperfine states $|F, m_F\rangle$ with large $|m_F|$ for qubit encoding, since $\Delta_{\text{vec}} \sim m_F$. For example, if Cs $|F=4, m_F=4\rangle$ and $|F=3, m_F=3\rangle$ states are used as qubit states $|1\rangle$ and $|0\rangle$, this will allow to increase to $\Delta_{\text{vec}} \sim 100 \times (m_F=4) \sim 400$ kHz, as a result the relative shift of the qubit state $|1\rangle$ in the left and right site is $2|\Delta_{\text{vec}}| \sim 800$ kHz. Choosing the same two-photon Rabi frequency $\Omega^2/\Delta \sim 40$ kHz, the last error term becomes $(7/8 + 19\pi^2/64)(\Omega^2/2\Delta|\Delta_{\text{vec}}|)^2 \sim 10^{-2}$. The Δ_{vec} can be increased even further using atoms with large hyperfine quantum numbers F , such as the rare-earth Ho, having $4 \leq F \leq 11$ in the ground $4f^{11}6s^2(^4I_{15/2})$ state [25], which will allow to increase to $\Delta_{\text{vec}} \sim 1$ MHz and reduce the corresponding error down to $\sim 10^{-3}$. The error $2\pi^2\langle(\delta\Omega/\Omega)^2\rangle = \pi^2(ka)^2 \left(1 - \sqrt{(1 + V_0/4V_1)/2}\right) / \left(1 + \sqrt{(1 + V_0/4V_1)/2}\right)$ due to the spread of the Rabi frequency experienced by each atom in a pair is harder to reduce, since it pretty much depends only on the ratio V_0/V_1 , which cannot be increased much beyond $V_0 \sim V_1$ in order to have motional states localized in left and right sites of a double-well. Using a very deep lattice with $V_0 = 200E_R$ and $V_0 = 2V_1$, which still results in motional states localized in the left and right sites, allows to reduce the error to $5 \cdot 10^{-2}$.

3. Lattice manipulation

In the previous subsection we showed how a phase gate can be applied to pairs of atoms in double-wells. To proceed with the cluster-state generation the phase gate has to be realized with the neighboring atoms in different double-wells, *i.e.* between each atom in a right site of the n^{th} double-well and an atom in a left site of the $(n+1)^{\text{th}}$ double-well. The phase gate operations described in the previous subsection can be applied if the atoms are brought to the same double-well. This can be achieved by adiabatically manipulating the lattice in the following way: (i) decreasing V_0 (Fig. 4b, left panel) which rises the barrier in each double-well, (ii) ramping the phase ϕ from 0 to $\pi/2$ (Fig. 4c, left panel), (iii) finally, increasing V_0 back to its initial value. As a result, the atoms that were in the right and left sites of neighboring double-wells end up in the same double-well (Fig. 4d, left panel).

The lattice manipulation has to be adiabatic to avoid motional excitation of atoms. Modeling the evolution of the atomic motional state during the lattice manipulation requires calculation of Bloch bands and Bloch functions for every configuration of the lattice. These are the eigenstates and eigenfunctions of the single-particle atomic Hamiltonian, which can be found by solving the Schrödinger equation with the potential $V(x, t)$. The potential $V(x, t)$ is periodic, and can be written as a discrete Fourier sum, containing terms with wavevectors

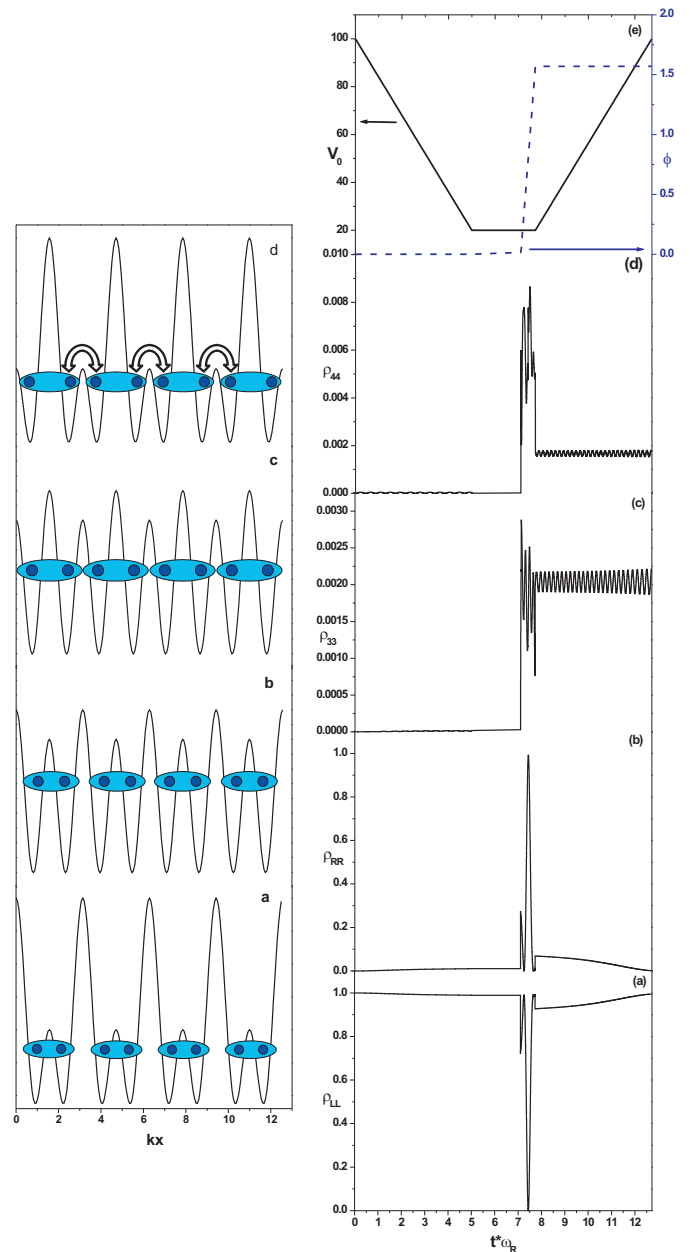


FIG. 4: Left panel: (a) Double-well lattice described by the potential $V = V_0 \cos^2(kx + \phi) + V_1 \cos^2(2kx)$, $V_1 = V_0$, $\phi = 0$; (b) V_0 is ramped down to $V_0 = 0.2V_1$; (c) The lattice phase is shifted from 0 to $\phi = \pi/2$, $V_0 = 0.2V_0$; (d) V_0 is ramped up to $V_0 = V_1$; Right panel: populations of the four lowest motional states during the V_0 and ϕ manipulations.

$k_x = \pm k, \pm 2k$, in the following way:

$$V(x, t) = (V_0 + V_1)/2 + V_0(e^{2ikx+2i\phi} + e^{-2ikx-2i\phi})/2 + V_1(e^{4ikx} + e^{-4ikx})/2,$$

allowing one to write the solutions of the Schrödinger equation in the form of Bloch functions $\psi_q^{(n)}(x) = e^{iqx}u_q(x)$. Here q is the quasi-momentum (restricted to

the first Brillouin zone), n is the band index, and

$$u_q(x) = \sum_{n=-N_{\max}}^{N_{\max}} c_n(q) e^{2inkx}, \quad (2)$$

with N_{\max} a suitable cutoff number. The resulting system of equations for the c_n coefficients and eigenenergies $E^{(n)}(q)$

$$\frac{\hbar^2(q + 2nk)^2}{2m} c_n + \frac{V_0}{2} (c_{n+1} e^{-2i\phi} + c_{n-1} e^{2i\phi}) + \frac{V_1}{2} (c_{n+2} + c_{n-2}) = (E^{(n)}(q) - \frac{V_0 + V_1}{2}) c_n,$$

is solved numerically by truncating the sum in Eq.(2) at some N_{\max} providing a necessary precision for the eigenenergies. We used $N_{\max} = 10$ to calculate the lowest Bloch energies and functions. Different configurations of the double-well potential and the corresponding band structures are shown in Fig. 5, where in the right panel of the figure the energies of the $q = 0$ eigenstates of each band are shown, since the lowest bands weakly depend on q . Given the Bloch functions $\psi_q^{(n)}$, which are delocalized over the entire lattice, one can construct Wannier functions which are localized at lattice sites x_i

$$w^{(n)}(x - x_i) = \frac{1}{\sqrt{N}} \sum_q e^{-iqx_i} \psi_q^{(n)}(x). \quad (3)$$

In a double-well lattice the two lowest bands are separated in energy by much less ($\leq 0.1E_R$) than the typical motional excitation energy $\sim \sqrt{4V_0E_R}$. As a result, even at ultracold temperatures both bands are going to be populated. In this situation to obtain a correct description of the system evolution generalized Wannier functions are introduced [23], which are superpositions of the Wannier functions of different energy bands. In our case the Bloch functions for the first two bands are symmetric (ground band) and anti-symmetric (second band) around the center of a double-well (shown in Fig. 6a). Combining the Wannier functions corresponding to the two bands as $\psi_{L,i} = (\psi_{1,i} - \psi_{2,i})/\sqrt{2}$ and $\psi_{R,i} = (\psi_{1,i} + \psi_{2,i})/\sqrt{2}$, one can obtain generalized Wannier functions localized in the left and right well, respectively (see Fig. 6b).

The lattice parameters have to be changed adiabatically to avoid undesirable motional excitations of the atoms, i.e., slow compared to the lattice motional energies. We checked the adiabaticity of lattice manipulation by numerical modeling of the system evolution. We took into account first four Bloch states to simplify the analysis and assumed that initially atoms are in the ground Bloch state. As we already mentioned, the lowest Bloch bands weakly depend on the quasi-momentum q , and, as a result, one can approximate the corresponding Wannier functions by the Bloch functions $\psi_{L,i}$ and $\psi_{R,i}$, restricted to a single site. The population evolution is shown in the right panel of Fig. 4, along with the time-dependence of the amplitude V_0 and phase ϕ . By optimizing the manipulation time we found that 99.92% of the population

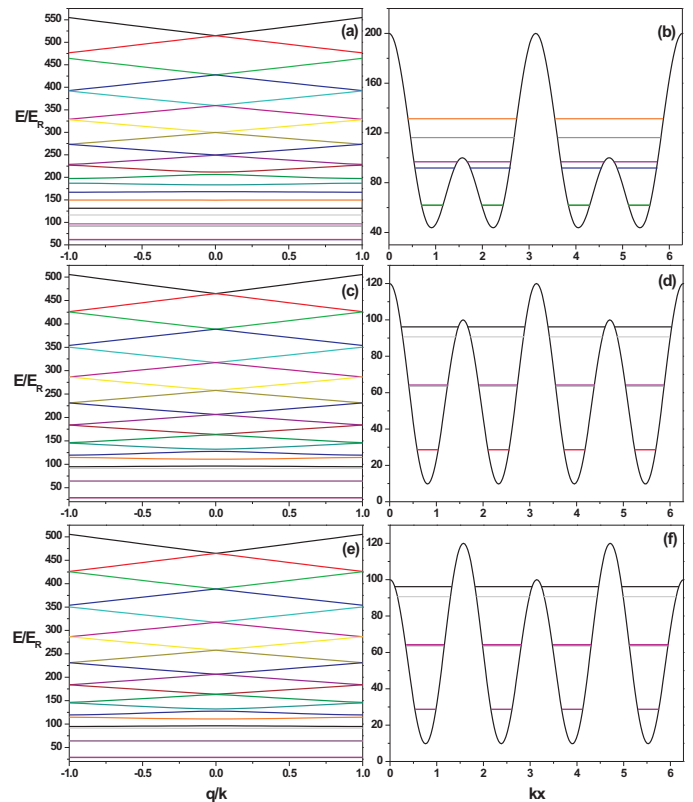


FIG. 5: Left panel: Bloch bands of the double-well lattice $V = V_0 \cos^2(kx + \phi) + V_1 \cos^2(2kx)$, (a) $V_1 = V_0 = 100E_R$, $\phi = 0$; (c) $V_0 = 0.2V_1$, $\phi = 0$; (e) $V_0 = 0.2V_0$, $\phi = \pi/2$; Right panel: Double-well potential along with lowest Bloch energies, where V_0 and ϕ in (b), (d) and (f) are the same as in the left panel for (a), (c) and (e).

stays in the ground Bloch band. We note that this value can be further increased by using more complex (optimized) functions $V_0(t)$ and $\phi(t)$. The total time required for the manipulation is $\sim 600 \mu\text{s}$.

We can now estimate the time required to generate a 1D cluster state. In the case considered in Section I A, when atoms are not addressed individually, the phase gate has to be performed adiabatically with the gate time $T_{\text{PG}} \gg 1/\omega \sim 1 \mu\text{s}$, as a result, the excitation-deexcitation pulses have to be longer than $10 \mu\text{s}$. We can assume the phase gate duration $T_{\text{PG}} \sim 20 \mu\text{s}$. The resulting time of cluster state generation, including four phase gate sequences is then $T_{1D} \sim 80 \mu\text{s}$. If atoms are not individually addressable, the gate duration was found to be $\sim 50 \mu\text{s}$ in Section I B. The total time including the lattice manipulation is then $T_{1D} \sim 800 \mu\text{s}$.

III. 2D CLUSTER STATE GENERATION

The scheme described in the previous section can be extended to generate a 2D cluster state, which is required

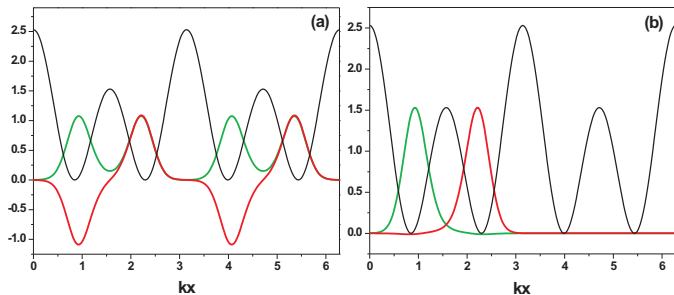


FIG. 6: (a) Bloch functions ψ_1 (green dot-dashed curve) and ψ_2 (red dashed curve) of the first and second Bloch bands along with the lattice potential $10^{-2}V$; (b) Wannier functions centered in the left $\psi_{L,i} = (\psi_{1,i} - \psi_{2,i})/\sqrt{2}$ and right $\psi_{R,i} = (\psi_{1,i} + \psi_{2,i})/\sqrt{2}$ sites of a double-well.

for universal quantum computation. First, atoms can be loaded in a 2D lattice with $V = V_0 \cos^2(k_1x + \phi) + V_1 \cos^2(2k_1x) + V_2 \cos^2(2k_2y)$, which produces a regular lattice with a period π/k_2 in y direction and a regular or double-well lattice in x direction. The y -lattice period is assumed sufficiently large so that atoms in neighboring x -chains do not interact when excited to Rydberg states. In this way, following the steps of Sections IA or IB, we can produce a series of 1D cluster states in the x direction. As a next step we adiabatically reduce V_1 to get a regular lattice in the x -direction with a period $\pi/2k_1$ (in the case of a double-well lattice), followed by stretching of the x -lattice. Next, the y -lattice period is reduced to bring the x -chains closer and the regular or double-well lattice $V = V_2 \cos^2(2k_2y + \phi) + V_3 \cos^2(k_2y + \phi)$ is switched on in the y direction. Next, the entanglement operations of Sections IA or IB can be repeated for 1D chains in the y direction, producing a 2D cluster state.

Let us estimate the time required to generate the 2D state. As we showed in the end of Section IC a 1D cluster state in the x -direction requires $T_{1D} \sim 100 \mu\text{s}$ without and $T_{1D} \sim 1 \text{ ms}$ with individual addressing in a pair to be realized. Adiabatic reduction of V_0 will take $\sim 250 \mu\text{s}$, as can be seen from Fig. 4(e) in the right panel. Next, we need to estimate the time required to stretch the x -lattice. The stretch has to be adiabatic for atoms to remain in the ground motional state of the lattice. We modeled the stretch of the lattice $V = V_1 \cos^2(2k_1x)$ so that the k vector was adiabatically changed from $2k_1$ to $0.4k_1$. The period of the lattice $5\pi/2k_1$ at the end of the stretch is comparable to the distance $3\pi/2k_1$ between atoms which belong to every other excited pair in the double-well. As a result, the error due to the interaction of atoms in neighboring x -chains is smaller than the error due to the interaction of atoms in neighboring excited pairs in the same chain.

We modeled the evolution of the system by calculating the Bloch bands and Bloch functions, and used the latter to construct single-site Wannier functions of the

lattice $V(x, t)$ during the stretch. We again took into account four lowest Bloch bands, assumed that initially the population was in the ground Bloch band, and monitored the excitation to higher-energy bands. We found that the stretch can be performed rather fast in $\sim 16/\omega_R \sim 730 \mu\text{s}$ while retaining 99.55% of the population in the ground Bloch band. The populations of the lowest four bands during the lattice stretch are shown in Fig. 7.

Finally, we can estimate the total time required to generate the 2D cluster state. The time required for 1D state generation $T_{1D} \sim 1 \text{ ms}$; ramping down the V_0 lattice takes $\sim 250 \mu\text{s}$ and the lattice stretch in the x -direction takes $\sim 730 \mu\text{s}$; the total time is $\sim 2 \text{ ms}$. Next, the lattice period of the lattice in the y -direction has to be adiabatically reduced, which will similarly take $\sim 730 \mu\text{s}$, followed by ramping up the V_3 lattice in $\sim 250 \mu\text{s}$, and a sequence of phase gate operations applied to the y -chains, will take $T_{1D} \sim 1 \text{ ms}$. Therefore, the total time of the 2D cluster state generation is $T_{2D} \sim 4 \text{ ms}$.

IV. CONCLUSIONS

We propose and analyze generation of a cluster state for measurement-based quantum computing with neutral atoms and polar molecules in an optical lattice using van der Waals and dipole-dipole interactions. We consider two schemes for implementation of a phase gate between pairs of nearest neighbors required to generate the cluster state: without and with individual addressing within a pair. We show that in the former case the gate error $\sim 7.2 \cdot 10^{-3}$ is feasible, provided the excitation-deexcitation to interacting states is adiabatic with respect to motional frequency of the lattice, which makes the scheme compatible with the fault-tolerance requirement of $7.5 \cdot 10^{-3}$ error for the phase gate of [24]. In the latter case individual addressing within a pair allows to implement the phase gate using Rydberg (dipole) blockade. Addressing of atoms within a pair can be realized in a polarization-gradient double-well lattice. The gate error in this case is ~ 0.335 and exceeds the fault-tolerance threshold, but can be reduced using atoms with large hyperfine quantum numbers, such as cesium and holmium, providing large vector shifts of hyperfine states. The error can be reduced even further to $5 \cdot 10^{-2}$ using a very deep optical lattice. We also analyze the lattice manipulation required in the former case to realize the phase gate between all nearest neighbors and show under which conditions the manipulation is adiabatic. The total time required to produce a 1D cluster state $T_{1D} \sim 100 \mu\text{s}$ without and $T_{1D} \sim 1 \text{ ms}$ with individual addressing in a pair, where parameters of ^{87}Rb were used for the estimate.

Finally, we showed how the scheme for 1D cluster state generation can be extended to realize a universal 2D cluster state and estimate the total time required $T_{2D} \sim 1.7 \text{ ms}$ without and $T_{2D} \sim 4 \text{ ms}$ with individual addressing in a pair.

The same scheme can be applied to generate the cluster

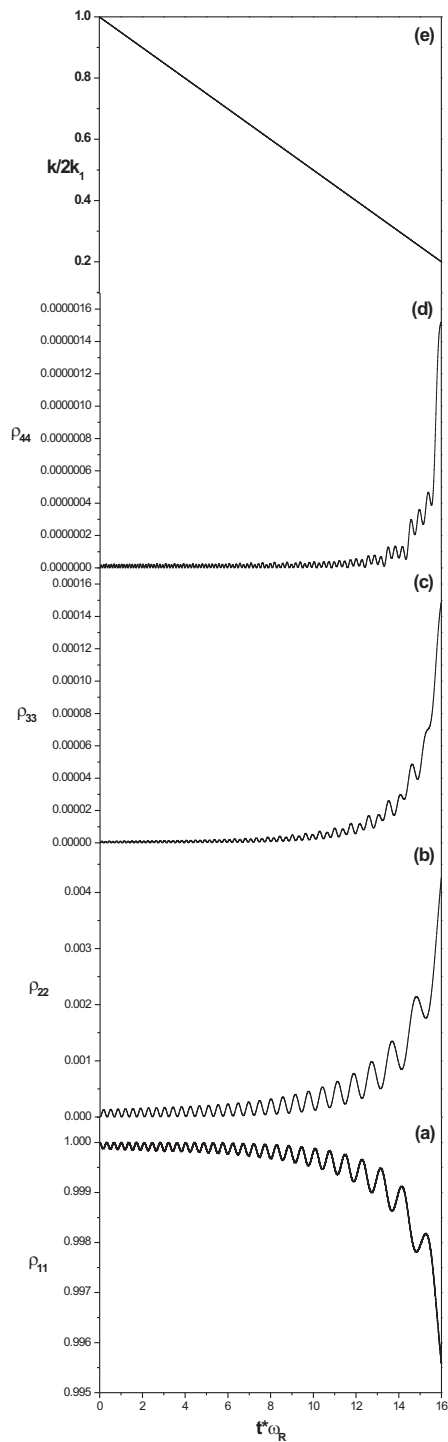


FIG. 7: (a)-(d) Populations of the four lowest Bloch bands during the lattice stretch; (e) the k vector is linearly reduced from $2k_1$ to $0.4k_1$.

state with polar molecules. For example, molecular states with small dipole moments can be used to encode a qubit while for the phase gate molecules can be excited to a state with a large dipole moment, such that in this state molecules can interact via dipole-dipole interaction. A good candidate is ^{13}CO [26], where the ground electronic state has a rather small permanent dipole moment ≈ 0.1 D and long-lived nuclear spin sublevels can be used to encode a qubit. It also has a metastable $a^3\Pi_0$ state with a significant permanent dipole moment ≈ 1.4 D, in which molecules can interact via dipole-dipole interaction.

V. ACKNOWLEDGMENTS

The authors gratefully acknowledge financial support from AFOSR under the MURI award FA9550-09-1-0588.

[1] M. A. Nielsen, I. L. Chuang, *Quantum Computation and Quantum Information*, Cambridge Univ. Press, Cam-

bridge, UK, 2000.

[2] N. Gisin, G. Ribordy, W. Tittel, H. Zbinden, *Rev. Mod.*

- Phys. **74**, 145 (2002).
- [3] C.F. Roos, M. Chwalla, K. Kim, M. Riebe, R. Blatt, Nature **443**, 316 (2006).
- [4] R. Raussendorf, H. J. Briegel, Phys. Rev. Lett. **86**, 5188 (2001); H. J. Briegel, R. Raussendorf, Phys. Rev. Lett. **86**, 910 (2001).
- [5] R. Raussendorf, D. E. Browne, H. J. Briegel, Phys. Rev. A **68**, 022312 (2003).
- [6] P. Walther, K. J. Resch, T. Rudolph, E. Schenck, H. Weinfurter, V. Vedral, M. Aspelmeyer, A. Zeilinger, Nature **434**, 169 (2005); C.-Y. Lu, X.-Q. Zhou, O. Cühne, W.-B. Gao, J. Zhang, Z.-S. Yuan, A. Goebel, T. Yang, J.-W. Pan, Nat. Phys. **3**, 91 (2007).
- [7] D. Gonta, T. Radtke, S. Fritzsche, Phys. Rev. A **79**, 062319 (2009).
- [8] H. Wunderlich, C. Wunderlich, K. Singer, F. Schmidt-Kaler, Phys. Rev. A **79**, 052324 (2009); R. Sock, D. F. V. James, Phys. Rev. Lett. **102**, 170501 (2009).
- [9] M. Zwiernik, P. Kok, Phys. Rev. A **79**, 022304 (2009).
- [10] O. Mandel, M. Greiner, A. Widera, T. Rom, T. W. Hansch, I. Bloch, Nature **425**, 937 (2003).
- [11] T. F. Gallagher, *Rydberg atoms*, Cambridge University Press, Cambridge (1994).
- [12] D. Jaksch, J. I. Cirac, P. Zoller, S. L. Rolston, R. Côté, M. D. Lukin, Phys. Rev. Lett. **87**, 037901 (2001);.
- [13] M. Saffman, T. G. Walker, K. Molmer, arXiv:0909.4777 (2009)
- [14] E. Urban, T. A. Johnson, T. Henage, L. Isenhower, D. D. Yavuz, T. G. Walker, M. Saffman, Nat. Phys. **5**, 110 (2009); T. Wilk, A. Gaetan, C. Evellin, J. Wolters, Y. Miroshnychenko, P. Grangier, A. Browayes, Phys. Rev. Lett. **104**, 010502 (2010).
- [15] L. Isenhower, E. Urban, X. L. Zhang, A. T. Gill, T. Henage, T. A. Johnson, T. G. Walker, M. Saffman, Phys. Rev. Lett. **104**, 010503 (2010).
- [16] T. Wilk, A. Gaetan, C. Evellin, J. Wolters, Y. Miroshnychenko, P. Grangier, A. Browayes, Phys. Rev. Lett. **104**, 010502 (2010).
- [17] C. Weitenberg, M. Endres, J. F. Sherson, M. Cheneau, P. Schaub, T. Fukuhara, I. Bloch, S. Kuhr, arXiv:1101.2076 (2011).
- [18] M. Saffman, T. G. Walker, Phys. Rev. A **72**, 022347 (2005).
- [19] J. Dalibard, C. Cohen-Tannoudji, J. Opt. Soc. Am. B **6**, 2033 (1989); J. Sebby-Strabley, M. Anderlini, P. S. Jessen, J. V. Porto, Phys. Rev. A **73**, 033605 (2006).
- [20] P. J. Lee, M. Anderlini, B. L. Brown, J. Sebby-Strabley, W. D. Phillips, J. V. Porto, Phys. Rev. Lett. **99**, 020402 (2007).
- [21] T. Calarco, U. Dorner, P. S. Julienne, C. J. Williams, P. Zoller, Phys. Rev. A **70**, 012306 (2004).
- [22] M. Lundblad, J. M. Obrecht, I. B. Spielman, J. V. Porto, Nat. Phys. **5**, 575 (2009).
- [23] B. Vaucher, S. R. Clark, U. Dorner, D. Jaksch, New J. Phys. **9**, 221 (2007).
- [24] R. Raussendorf, J. Harrington, K. Goyal, New J. Phys. **9**, 199 (2007).
- [25] M. Saffman, K. Molmer, Phys. Rev. A **78**, 012336 (2008).
- [26] E. Kuznetsova, K. Rirby, R. Côté, S. F. Yelin, Phys. Rev. A **78**, 012313 (2008).